Clover – Measuring the CMB *B*-mode polarisation

C. E. North[1], P. A. R. Ade[2], M. D. Audley[3], C. Baines[4], R. A. Battye[4], M. L. Brown[3], P. Cabella[1], P. G. Calisse[2], A. D. Challinor[5,6], W. D. Duncan[7], P. Ferreira[1], W. K. Gear[2], D. Glowacka[3], D. J. Goldie[3], P. K. Grimes[1], M. Halpern[8], V. Haynes[4], G. C. Hilton[7], K. D. Irwin[7], B. R. Johnson[1], M. E. Jones[1], A. N. Lasenby[3], P. J. Leahy[4], J. Leech[1], S. Lewis[4], B. Maffei[4], L. Martinis[4], P. Mauskopf[2], S. J. Melhuish[4], D. O'Dea[3,5], S. M. Parsley[2], L. Piccirillo[4], G. Pisano[4], C. D. Reintsema[7], G. Savini[2], R. Sudiwala[2], D. Sutton[1], A. C. Taylor[1], G. Teleberg[2], D. Titterington[3], V. Tsaneva[3], C. Tucker[2], R. Watson[4], S. Withington[3], G. Yassin[1], J. Zhang[2]

Abstract— **We describe the objectives, design and predicted performance of Clover, a fully-funded, UK-led experiment to measure the *B*-mode polarisation of the Cosmic Microwave Background (CMB). Three individual telescopes will operate at 97, 150 and 225 GHz, each populated by up to 256 horns. The detectors, TES bolometers, are limited by unavoidable photon noise, and coupled to an optical design which gives very low systematic errors, particularly in cross-polarisation. The telescopes will sit on three-axis mounts on a site in the Atacama Desert. The angular resolution of around 8´ and sky coverage of around 1000 deg^2 provide multipole coverage of $20<\ell<1000$. Combined with the high sensitivity, this should allow the *B*-mode signal to be measured (or constrained) down to a level corresponding to a tensor-to-scalar ratio of $r = 0.01$, providing the emission from polarised foregrounds can be subtracted. This in turn will allow constraints to be placed on the energy scale of inflation, providing an unprecedented insight into the early history of the Universe.**

I. Introduction

Measurement of the cosmic microwave background (CMB) polarisation can provide information about the early universe not available from other observations alone. It will provide further constraints on cosmological parameters and break some of the existing degeneracies between them (see e.g. [1],[2]). The CMB fluctuations are polarised at about the 10% level. The polarisation field can be decomposed into two modes: the *E*-mode, a "grad-like" mode with even parity; and the *B*-mode, a "curl-like" mode with odd parity.

The primordial density perturbations which give rise to the large scale structure of matter in the Universe dominate the temperature anisotropies. These scalar perturbations generate only an *E*-mode polarisation with an r.m.s. of ~5 μK. The *E*-mode power spectrum and its correlation to the temperature power spectrum have been measured by several experiments

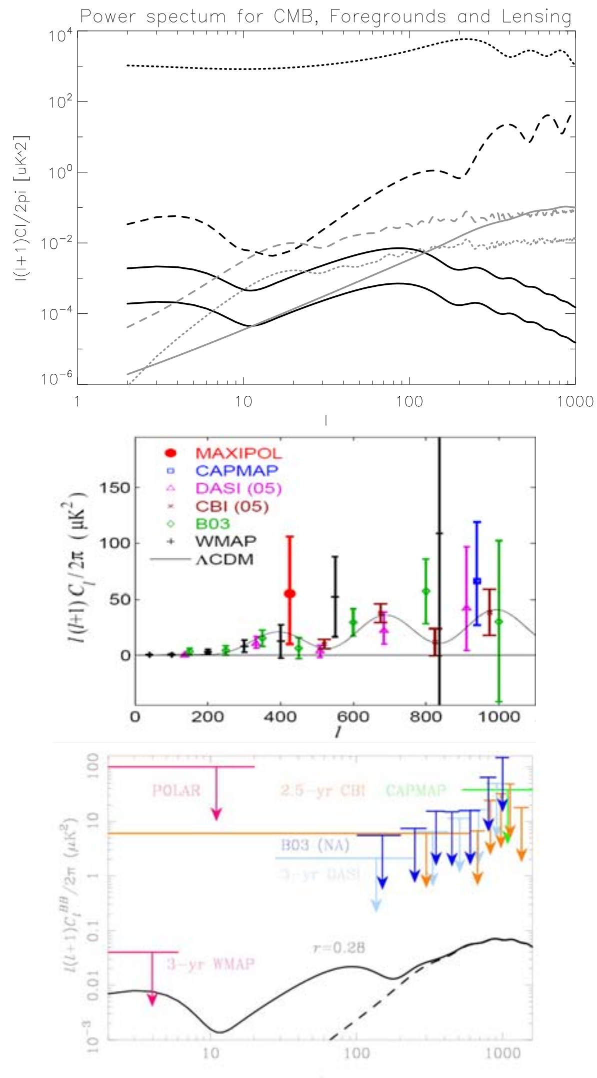

Figure 1: Top: Angular power spectrum of the CMB, showing the power in the spherical harmonics associated with multipole l (where $l \approx 180°/\theta$). Shown are the temperature (black dotted), *E*-mode (black dashed) and *B*-mode (black solid; upper: $r = 0.1$, lower: $r = 0.01$) for the CMB. For comparison, we show the *B*-mode from weak gravitational lensing (grey solid), as well as galactic synchrotron (grey dashed) and thermal dust (grey dotted) emission at 100 GHz. The levels of the galactic emission are based on very simple models, so are for rough comparison only, and are calculated in regions of low emission. Bottom left: current *E*-mode power spectrum results compared with the ΛCDM model (from [5]). Bottom right: current limits on the *B*-mode power spectrum compared with a model for $r = 0.28$ (solid black line) and the weak lensing contamination (dashed line).

[1] Oxford Astrophysics, University of Oxford, UK
[2] School of Physics and Astronomy, Cardiff University, UK
[3] Cavendish Laboratory, University of Cambridge, Cambridge, UK
[4] School of Physics and Astronomy, University of Manchester, UK
[5] Institute of Astronomy, University of Cambridge, UK
[6] DAMTP, University of Cambridge, UK
[7] National Institute of Standards and Technology, USA
[8] University of British Columbia, Canada

This paper describes the current design for Clover, which is currently under review and may change in the future.

(e.g. [3],[4],[5]).

Theories of inflation predict the quantum generation of primordial gravitational waves and these propagated through the early universe, further polarising the CMB. These tensor perturbations cause both *E*-mode and *B*-mode signals, but at much lower level than the scalar perturbations. Measurement of the *B*-mode signal due to gravitational waves would allow direct measurement of the tensor-to-scalar ratio, r, the value of which can be linked directly to the energy scale of inflation. Measuring the value (or upper limit) of this would thus place constraints on inflationary theories.

Current measurements constrain r to less than 0.28 [6]. For $r = 0.01$, the *B*-mode signal is around 10 nK, so excellent control and knowledge of systematic effects is required for its detection.

Spurious *B*-mode signals are cause by both astrophysical and systematic effects. Astrophysical signals include extragalactic point sources, as well as diffuse galactic synchrotron and thermal dust emission. Weak gravitational lensing of the *E*-mode signal also causes spurious *B*-mode signal, which exceeds the primordial signal on small angular scales (see Figure 1).

Clover is a project intended to measure the *B*-mode polarisation of the CMB. It is a collaboration between the Universities of Oxford, Cambridge, Cardiff and Manchester. Detector readout technology is supplied by the University of British Columbia (UBC) and the National Institute of Standards and Technology (NIST). Clover will comprise three telescopes operating at central frequencies of 97, 150 and 225 GHz with 30% bandwidth. The spectral coverage is intended to allow separation of the CMB from the foreground contaminants. Each telescope will have a Compact Range Antenna optical system, which gives exceptionally low aberrations and cross-polarisation across a large focal plane. Each focal plane will be populated with arrays of polarimeters. Each pixel consists of a horn directly coupled to two transition edge sensor (TES) detectors, one for each polarisation. The polarisation of each pixel will be rotated so that each individual detector will independently measure the Stokes parameters, I, Q and U, removing the need for detector differencing. The TESs give background-limited sensitivity and can be manufactured in large quantities using lithographic techniques.

The science goals of Clover are:

- Measure r, for $r > 0.01$, by characterizing the *B*-mode polarisation power spectrum.
- Make sample-variance limited measurements of the temperature, *E*-mode and *T-E* cross-correlation power spectra over ~1000 deg^2.
- Measure the *B*-modes from weak gravitational lensing.
- Improve constraints on cosmological parameters.
- Determine or constrain the energy scale of inflation.
- Characterise the polarised Galactic foregrounds in regions of low emission.

TABLE 1
INSTRUMENT REQUIREMENTS

Instrument Characteristic	Requirements
Stokes parameters measured	I, Q and U **at each detector**
Multipole range	$20 < l < 1000$
Resolution	8 arcmin
Sky area	1000 deg^2
Noise limit	Unavoidable photon noise
Detector NET at 97, 150, 225 GHz	150, 225, 590 μKs$^{0.5}$
Detector NEP at 97, 150, 225 GHz	2, 4, 8 x 10^{-17} WHz$^{-0.5}$
# Detectors at 97, 150, 225 GHz	338, 504, 504
Polarisation beam alignment	< 0.2% FWHM
Average beam ellipticity	< 0.85
Differential eccentricity[a]	< 0.012
Residual Q↔U rotation (cross-pol)	< 0.24° (< 1.4%)
Q,U loss (depolarization)	< 10%
Residual T→Q,U mixing (depolarization)	< 0.015%
Polarisation modulation efficiency	90%
Absolute Calibration	5%

[a] Differential eccentricity is the difference in eccentricity between beams of the two orthogonal polarisations.

II. INSTRUMENT DESCRIPTION

A. Requirements

The ambitious science goals of Clover mean that the instrument requirements are very stringent. Some of the requirements are listed in Table 1. The particularly stringent optics requirements are the $Q \leftrightarrow U$ rotation (cross-polarisation), the differential eccentricity, and the residual $T \rightarrow Q,U$ mixing (instrumental polarisation).

B. Optics

The Compact Range Antenna optical design of Clover [7] gives excellent cross-polarisation performance and low aberrations, as shown in Figure 3 for the 97 GHz. The large, flat focal plane means that the edge pixels have poorer performance than the central pixel, but these still meet the requirements given in Table 1. Sidelobes caused by diffraction around the mirrors are absorbed by the co-moving ground shield. The sidelobe at -50° (bottom panel of Figure

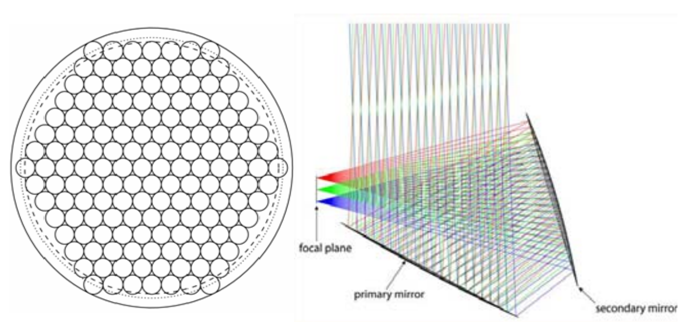

Figure 2: Left: layout of the 97 GHz hex-packed focal plane array. Right: optics ray diagram, showing the parabolic primary mirror, hyperbolic secondary mirror and the flat focal plane. The field of view of the whole array is around 2°.

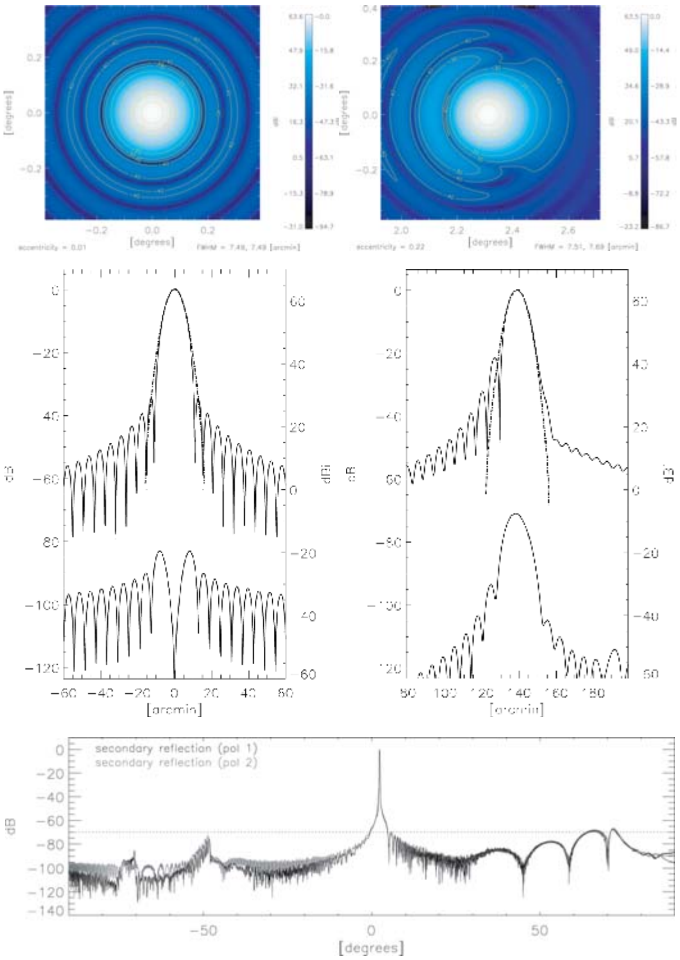

Figure 4: 97 GHz Optics performance. Top row: Beam maps of the central feed (left) and an edge feed (right). Middle row: Main beam cuts of the central feed (left) and an edge feed (right), showing the co-polar (top solid line), cross-polar (bottom solid line) and Gaussian approximation (dot-dashed line). Bottom: Far sidelobes of an edge pixel, up to 100° either side of the main beam for both polarisations.

3) is caused by an additional reflection off the secondary mirror.

The 97 GHz mirrors will both be around 1.8 m in diameter. The primary mirror has an offset parabolic shape, and the secondary mirror is an offset inverse (i.e. concave) hyperboloid.

C. Polarimeter

Each pixel in the array comprises a single feed horn directly coupled to two TES detectors. Between the two will be an Orthomode Transducer (OMT), which splits the signal into two orthogonal polarizations. In front of the focal plane will be a single achromatic half-wave plate (AHWP) [8],[9]. This is a stack of three sapphire plates forming a birefringent layer. When rotated at angular speed ω, the polarisation angle of the incoming radiation is rotated in such a way that the outputs of the two detectors are:

$$\begin{aligned} D_1(t) &= I - Q\cos(4\omega t) - U\sin(4\omega t) \\ D_2(t) &= I + Q\cos(4\omega t) + U\cos(4\omega t) \end{aligned} \qquad (1)$$

Rotating the AHWP ensures that each detector measures both Q and U, modulated as shown in (1).

D. Feed Horns

The requirement on the horns is that they have cross-polarisation below -30dB, sidelobes below -25dB and average return loss below -20dB. The chosen design is an electroformed, corrugated, Winston-like profile horn. At 97 GHz the horns have an aperture diameter of around 18 mm and a length of around 70 mm. At 150 and 225 GHz, the apertures are scaled by frequency to around 10 mm and 8 mm respectively. Measurements of prototype horns have shown excellent agreement to models, as shown in Figure 4.

E. Orthomode Transducers

At 97 GHz, the OMT will be an electroformed turnstile junction OMT [10]. This design accepts circular waveguide input and outputs perpendicular polarisations into rectangular waveguide. Prototype measurements have confirmed that the OMT has better than -20dB return loss and below -40dB isolation between the two outputs (i.e. cross-polarisation). The rectangular waveguide outputs are coupled to the detector chips through a finline transition (see below).

At 150 and 225 GHz the OMT will be a cylindrical waveguide with four rectangular probes. Signals from opposite probes will be combined in planar circuitry and then connected directly to the TES detectors. This has the advantage that the rectangular probe OMT and TES detectors can be on the same chip. Simulations have predicted a return loss of -20dB and isolation of -60dB. Scale models are currently being designed and tested.

F. Finline Transition

The rectangular waveguide output of the 97 GHz OMT is transformed into microstrip using a finline transition [11],[12]. The finline chip, which has a 225 μm thick silicon substrate, sits across the middle of the waveguide, supported in a groove. "Fins" of 500 nm thick superconducting niobium (Nb) are tapered in smoothly until they overlap, forming antipodal finline. The structure behaves as unilateral finline when the distance between the fins is much larger than the 400 nm of SiO_2 separating them.

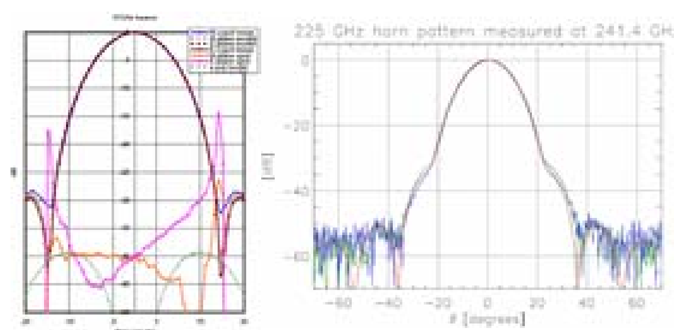

Figure 3: Measurements of prototype horns for 97 GHz (left) and 225 GHz (right) channels. Comparison to models is shown, with the data being indistinguishable from the models down to the -30dB level.

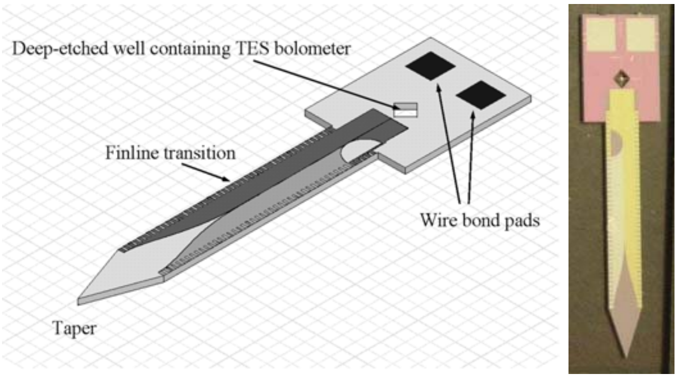

Figure 6: A schematic of the finline chip (left), and a photo of a prototype (right). The point at the end forms a transition from unloaded waveguide to waveguide loaded with Silicon. The TES detector sits in the diamond-shaped well at the end of the microstrip.

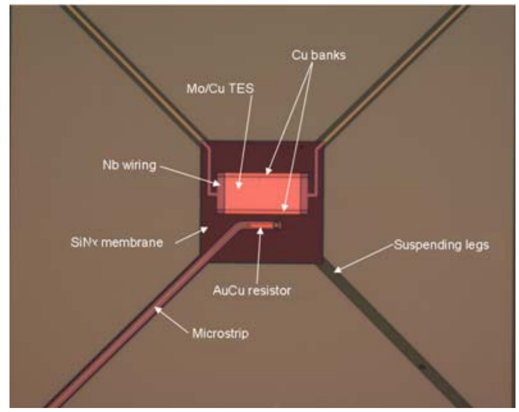

Figure 5: Schematic of the detector well, showing the microstrip terminating at the AuCu resistor and the Mo/Cu TES in the well. The nitrite suspension legs control the thermal conductance.

The transition from antipodal finline to microstrip is through a semicircular structure, where the outer edge of the top layer is brought in towards the centre (making the strip), then the inner edge of the bottom layer is brought out (forming the ground plane of the microstrip) (see Figure 6). Serrations of Nb sit in the waveguide groove to cut off other modes propagating in the waveguide. The 3 µm wide microstrip leads to a resistor on a SiN_x membrane in the deep-etched well, seen as the diamond shape in Figure 6.

G. Detectors and Readout

The Clover detectors are Mo/Cu TES bolometers [13] sitting on a 500 nm thick SiN_x membrane in a 660 µm square well in the substrate. The Nb microstrip input is terminated in an AuCu resistor (see Figure 5). Thermal conductance to the thermal bath is controlled by four nitride legs. The critical temperature of the TESs' transition, between superconducting and normal behaviour, is about 190 mK (430 mK for 220GHz). They are cooled to 100 mK (230 mK for 225 GHz) in order to achieve the target NEPs (see Table 1). The chips are manufactured on Si wafers and cut into individual devices using Deep Reactive Ion Etching (DRIE) to ensure 100% cover of the focal plane. Prototype measurements have shown that the TES films are of high quality, and the devices have an electrical NEP close to the phonon noise level. While the thermal conductance of the nitride legs needs to be adjusted to achieve the required power handling, the prototype results show that the detectors have sharp resistance changes at the superconducting transition (α=500 for $\log(R)=\alpha.\log(T)$) and fast rise times ($1/e$ rise times of ~150 µs).

The readout and subsequent amplification is provided by a three-stage SQUID system. The MUX chips will all connect to Multi-channel electronics (MCE) supplied by UBC. The 32x1 multiplexer (MUX) chips supplied by NIST [14],[15],[16] lend themselves to linear arrangements of detectors. For this reason, the focal plane is split into rows, with 22 rows making up the 97 GHz focal plane. Each row of 16–20 detectors will be held in a single split block (see Figure 8).

H. Cryogenics

The base temperature at which the detectors operate is reached by a three-stage (97 and 150 GHz) or two-stage (225 GHz) cryogenic system. The requirements on the cryogenic system are to provide 3 µW of cooling power at the base temperature. The temperature stability of the system must be 60 nK/Hz$^{0.5}$ with long-term stability of 3.5 µK over the 24 hour duty cycle. At 97 and 150 GHz, the system uses a CryoMech PT410 pulse tube cooler (PTC) to cool to 4 K, a closed-cycle He-7 sorption fridge down to 0.4 K, and a closed-cycle dilution refrigerator [17] to reach 100 mK. At 225 GHz there will again be a PT410 PTC, followed by a

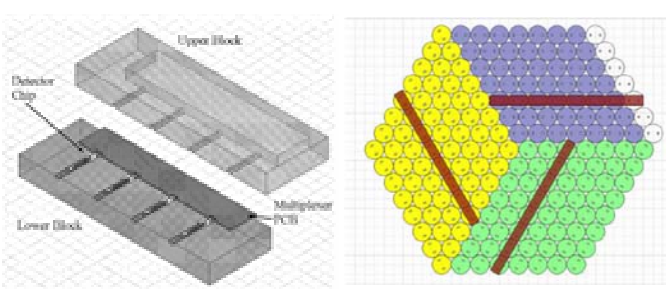

Figure 8: The design of the detector block at 97 GHz (left), and the concept behind the arrangement of the linear blocks in the focal plane (right). The two halves of the split block form the waveguide into which the finlines protrude.

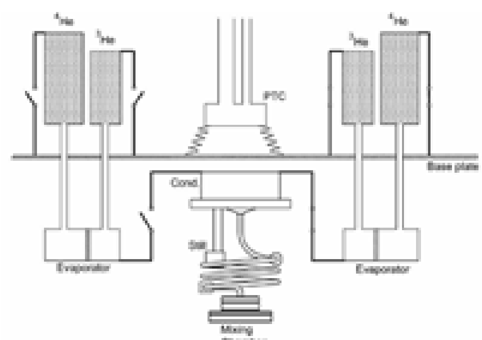

Figure 7: Schematic of the 97 GHz cryogenic system, showing the PTC (top middle), the sorption refrigerators (left and right), and the dilution refrigerator (bottom middle

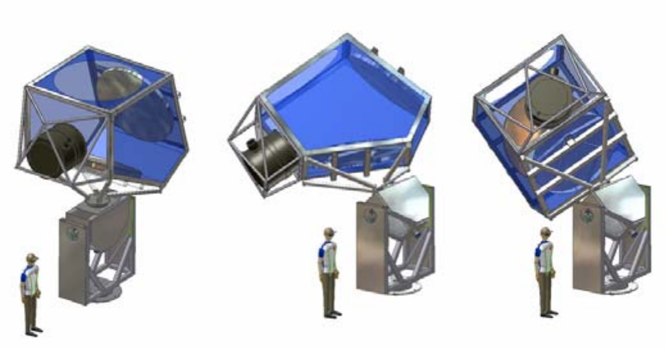

Figure 9: Three views of the 97 GHz mount showing its ability to rotate around three axes. The optical assembly, containing the 1.8 m mirrors, will be lined with an unpolarised absorber to reduce the effects of sidelobes.

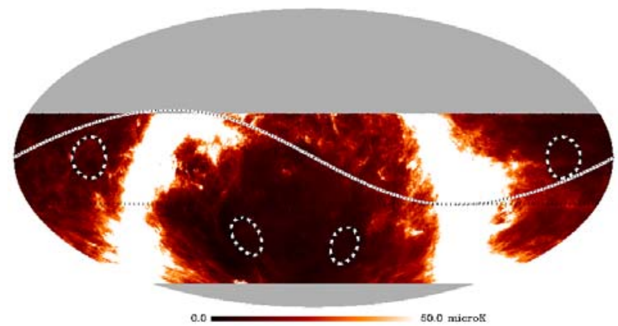

Figure 10: Mollweide projection of the sky in equatorial coordinates showing the Clover fields (black/white circles) relative to the site latitude (black line), the ecliptic plane (black/white dotted line) and the estimated galactic foreground emission at 97 GHz from toy models (greyscale).

He-10 sorption cooler to reach 250 mK. The closed-cycle nature means that there will be no cryogenic consumables. To reduce vibrations flexible stainless steel lines will lead to the PTC motor and expansion stage.

Band-pass and thermal filtering will be provided by a stack of metal-mesh filters. The maximum possible size of these filters (300 mm) is what limits the focal plane size, and hence the number of horns; this it the reason for the reduced number of horns at 97 GHz (169 rather than 202 at the higher frequencies).

I. Mount

Each telescope will have its own mount, with the sizes roughly scaled with the frequency. The mount must be rotate fully in azimuth and reach elevations from 0–89.5°. As a further modulation of the polarisation signal, the mount will rotate the telescope around the optical axis. To move the science signals away from the atmospheric noise, the mount must be able to scan at speeds of at least 3 deg.s^{-1} on the sky, and have sufficient acceleration to keep the turnaround time as low as possible (see below). The pointing accuracy must be 20 arcsec, with long-term tracking accuracy of 60 arcsec. The 97 GHz mount design (without counterweights for clarity) is shown in Figure 9.

III. Site and Observations

Clover will be sited at Llano de Chajnantor, Chile, in the Atacama Desert. The high altitude (5080 m) places it above nearly half the atmosphere and most of the water vapour. The area is a popular one for millimetre and sub-millimetre experiments (e.g. ALMA, CBI, ACT, CCAT, etc.), as it is very dry and still accessible.

The latitude of the site (-23°) means that a good proportion of the sky is observable. Since contamination from Galactic foregrounds is a major issue for CMB *B*-mode experiments, the ability to select locations out of the galactic plane is vital. The required 1000 deg^2 of sky area is divided into four convex fields, spread roughly evenly in right ascension to maximise the observing efficiency throughout the year (see Figure 10).

In order to control the atmospheric noise as much as possible, Clover will perform fast constant-elevation scans over each field as it rises and falls each night. The observations will continue for two years, giving ~0.8 years of integration time needed to achieve the final required sensitivity.

Calibration for CMB polarisation experiments is particularly challenging, as there are few well-characterised, polarised, non-variable astronomical sources at mm wavelengths. Possible sources are extragalactic radio sources (e.g. Tau A) and planets (though planets are not highly polarised). While an absolute calibration of 5% should be possible from existing or planned data (e.g. WMAP, Planck), it is likely that characterisation of systematic effects will require additional calibration, possibly from an artificial source.

IV. Data Analysis and Predictions

The fast detector speed and the large number of detectors mean that Clover will produce a very high volume of data. The usual data analysis procedures (e.g. deglitching, de-striping, etc.) will have to be applied to this data set in order to generate the final maps.

An additional challenge for *B*-mode experiments will be the removal of the foreground signals, particularly the galactic synchrotron and dust emission. The spectral coverage of Clover means that component separation should be possible, though it will probably require significantly more knowledge of the foregrounds than exists at the moment. For example, current data has a low signal-to-noise in the low emission areas of sky that we will target, and is either at too low a frequency (e.g. 1.4 GHz [18]) in the case of synchrotron emission or too high a frequency (e.g. 350 GHz [19] or 100 μm [20]) in the case of thermal dust emission. Much work is being done to make better predictions and observations of these signals (e.g. [21],[22]). Future all sky surveys at higher frequencies (e.g. CBASS at 5 GHz) will provide a lot of data on the synchrotron emission. This will also be at a frequency high enough to neglect Faraday rotation, which is a major problem when extrapolating from lower frequencies.

SUMMARY

Clover has a unique instrument design which provides excellent control of systematic errors. This is required to complete the main science goal of characterising the CMB *B*-mode signal due to gravitational waves from inflation. The sensitivity will be good enough to measure or constrain the *B*-modes down to a level corresponding to a tensor-to-scalar ratio of $r = 0.01$, providing the polarised foreground emission can be subtracted.

The 97 GHz Clover telescope is in the final stages of the design phase, and is planned to be on the site towards the end of 2008, and will be installed, commissioned and tested over the following year. The 150 GHz instrument is planned to be shipped in mid-2009 and the 225 GHz in late 2009.

ACKNOWLEDGMENT

Clover is funded by the Science and Technology Facilities Council. CEN acknowledges a STFC studentship.

REFERENCES

[1] W. Hu, M. White, 1997, *A CMB Polarization Primer*, New Ast., **2**, 323

[2] A. Challinor, 2005, *Constraining fundamental physics with the cosmic microwave background*, arXiv:astro-ph/0606548v1

[3] J. M. Kovac, E. M. Leitch, C. Pryke, J. E. Carlstrom, N. W. Halverson, W. L Holzapfel, 2002, *Detection of Polarization in the Cosmic Microwave Background using DASI*, Nature, **420**, 722

[4] J. L. Sievers, C. Achermann, J. R. Bond, et al., in press, *Implications of the Cosmic Background Imager Polarization Data*, arXiv:astro-ph/0509203v2

[5] J. H. P. Wu, J. Zuntz, M. E. Abroe, et al., in press, *MAXIPOL: Data Analysis and Results*, arXiv:astro-ph/0611392

[6] D. N. Spergel, R. Bean, O. Doré, et al., in press, *Wilkinson Microwave Anisotropy Probe (WMAP) Three Year Results: Implications for Cosmology*, arXiv: astro-ph/0603449v2

[7] G. Yassin, P. K. Grimes, S. B. Sorenson, 2005, Proc. of the 16th Int. Symp. on Space Terahertz Technology, Gothenburg, Sweden

[8] G. Savini, G. Pisano, P. A. R. Ade, 2006, *Achromatic half-wave plate for submillimeter instruments in cosmic microwave background astronomy: modeling and simulation*, Applied Optics, **45**, 35, 8907–8915.

[9] G. Pisano, G. Savini, P. A. R. Ade, V. Haynes W. K. Gear, 2006, *Achromatic half-wave plate for submillimeter instruments in cosmic microwave background astronomy: experimental characterization*, Applied Optics, **45**, 27, 6982–6989

[10] G. Pisano, L. Pietranera, K. Isaak, L. Piccirillo, B. R. Johnson, B. Maffei, S. Melhuish, 2007, *A Broadband WR10 Turnstile Junction Orthomode Transducer*, IEEE Microwave and Wireless Components Letters, **17**, 4, 286–288

[11] C. E. North, G. Yassin, P. K. Grimes, 2006, *Rigorous Analysis and Design of Finline Tapers for High Performance Millimetre and Submillimetre Detectors*, Proc. of the 17th Int. Symp. on Space Terahertz Technology, Paris, France, in press

[12] G. Yassin, S. Withington, M. Buffey, K. Jacobs, S. Wulff, 2000, *A 350 GHz SIS Antipodal Finline Mixer*, IEEE Trans. on Microwave Theory and Techniques, **48**, 662

[13] M. D. Audley, R. W. Barker, M. Crane, et al., 2006, *Prototype finline-coupled TES bolometers for CLOVER*, Proc. of the 17th Int. Symp. on Space Terahertz Technology, Paris, France, arXiv:astro-ph/0608285v1

[14] Reintsema, C.D, J. Beyer, S.W. Nam, S. Deiker, G.C. Hilton, K. Irwin, J. Martinis, J. Ullom,L.R. Vale, M. MacIntosh 2003, *A Prototype System for Time-Domain SQUID Multiplexing of Large-Format Transition-Edge Sensor Arrays*, Review of Scientific Instruments, **74**, 4500

[15] Chervenak, J.A., K.D. Irwin, E.N. Grossman, J.M. Martinis, C.D. Reintsema, and M.E. Huber 1999, *Superconducting multiplexer for arrays of transition edge sensors*, Applied Physics Letters, **74**, 4043—4045

[16] P.A.J. de Korte , J. Beyer , S. Deiker, G.C. Hilton, K.D. Irwin, M. MacIntosh , S.W. Nam, C.D. Reintsema, L.R. Vale and M.E. Huber 2003, *Time-Division SQUID Multiplexer for Transition-Edge Sensors, Review of Scientific Instruments*, **74**, 3807

[17] G. Teleberg, S. T. Chase, L. Piccirillo, 2006, *A miniature dilution refrigerator for sub-Kelvin detector arrays*, Proceedings of SPIE, **6275**, 62750D

[18] L. La Porta, C. Burigana, W. Reich, P. Reich, 2006, *An angular power spectrum analysis of the DRAO 1.4 GHz polarization survey: implications for CMB observations*, A&A, **455**, 2, L9 – L12

[19] N. Ponthieu, J. F. Macías-Pérez, M. Tristram, P. Ade, A. Amblard, et al., 2005, *Temperature and polarization angular power spectra of Galactic dust radiation at 353 GHz as measured by Archeops*, A&A, **444**, 327–336

[20] D. P. Finkbeiner, M. Davis, D. J. Schlegel, 1999, *Extrapolation of Galactic Dust Emission at 100 Microns to Cosmic Microwave Background Radiation Frequencies Using FIRAS*, ApJ, **524**, 2, 867–886

[21] C. Burigana, L. La Porta, W. Reich, et al., 2006, *Polarized Synchrotron emission*, Proc. of CMB and Physics of the Early Universe, Ischia, Italy, arXiv:astro-ph/0607469v1

[22] E. Carretti, G. Bernardi, S. Cortiglinoi, 2006, *B-mode contamination by synchrotron emission from 3-yr Wilkinson Microwave Anisotropy Probe data*, MNRAS, **373L**, 93C